KeAi

Contents lists available at ScienceDirect

Petroleum Science

journal homepage: www.keaipublishing.com/en/journals/petroleum-science



Original Paper

Ethoxylated molybdenum disulphide based nanofluid for enhanced oil recovery



Infant Raj, Zhuo Lu, Ji-Rui Hou*, Yu-Chen Wen, Li-Xiao Xiao

Unconventional Petroleum Research Institute, China University of Petroleum (Beijing), Beijing, 102249, China

ARTICLE INFO

Article history Received 8 November 2023 Received in revised form 14 August 2024 Accepted 21 August 2024 Available online 23 August 2024

Edited by Yan-Hua Sun

Keywords: Molybdenum disulfide Nanofluid Flow in porous media Core flooding Interfacial tension

ABSTRACT

Despite advances in renewable energy sources, the world's current infrastructure and consumption patterns still heavily depend on crude oil. Enhanced oil recovery (EOR) is a crucial method for significantly increasing the amount of crude oil extracted from mature and declining oil fields. Nanomaterials have shown great potential in improving EOR methods due to their unique properties, such as high surface area, tunable surface chemistry, and the ability to interact at the molecular level with fluids and rock surfaces. This study examines the potential use of incorporating ethoxylated molybdenum disulfide with a unique three-dimensional flower-like morphology for overcoming the challenges associated with oil recovery from reservoirs characterized by complex pore structures and low permeability. The synthesized nanomaterial features a chemical composition that encompasses a polar ethoxy group linking molybdenum disulfide nanosheets and an alkylamine chain. The ethoxy group promotes interactions with water molecules through hydrogen bonding and electrostatic forces, disrupting the cohesive forces among water molecules and reduction surface tension at the oil-water interface. As a result, the nanomaterial achieves an ultra-low interfacial tension of 10⁻³ mN/m. Core flooding experiments demonstrate a significant oil recovery of approximately 70% at a concentration as low as 50 ppm. This research paves the way for the design and synthesis of advanced extended surfactant-like nanomaterials, offering a promising avenue for enhancing oil recovery efficiency.

© 2024 The Authors. Publishing services by Elsevier B.V. on behalf of KeAi Communications Co. Ltd. This is an open access article under the CC BY-NC-ND license (http://creativecommons.org/licenses/by-nc-nd/

4.0/).

1. Introduction

Crude oil plays a crucial role in the global energy system, influencing economic activities, geopolitical strategies, and technological advancement. Nearly two-thirds of the oil remains trapped in reservoirs after primary and secondary recovery stages. Therefore, it is essential to implement further enhanced oil recovery (EOR) processes. The primary goal of EOR is to improve the overall recovery factor by modifying reservoir conditions, such as wettability and interfacial tension (IFT), and enhancing oil mobility using various chemicals (Deng et al., 2021; Eltoum et al., 2021; Kazemzadeh et al., 2019; Vats et al., 2023).

Nanomaterials have gained significant attention in EOR processes due to their economic and environmental benefits (Ahmadi et al., 2024; Halari et al., 2024; Motraghi et al., 2023; Pandey et al., 2022). Recent research has demonstrated that mixing

* Corresponding author. E-mail address: houjirui@cup.edu.cn (J.-R. Hou). nanoparticles with surfactants can reduce surface tension (Kesarwani et al., 2022a, 2022b; Manshad et al., 2024). However, their efficiency in oil recovery remains a major concern. Thus, alternative materials like graphene oxide and transition metal dichalcogenides (TMD) are being widely explored (Mirzavandi et al., 2023; Pandey et al., 2023; Raj et al., 2019).

TMD materials, a class of two-dimensional (2D) materials, have attracted considerable attention in nanotechnology and materials science. TMDs consist of transition metal atoms, such as molybdenum or tungsten, bonded to two chalcogen atoms, such as sulfur, selenium, or tellurium. They exhibit unique properties due to their two-dimensional layered structure, where each layer is only a few atoms thick (Chowdhury et al., 2020). Their semiconductor nature makes them promising for applications in electronics and optoelectronics, flexible electronics, photovoltaics, sensors, and transistors (Desai et al., 2016; Jiang et al., 2022; Mackin et al., 2020; Tan et al., 2020; Xu et al., 2016). Additionally, their mechanical, thermal, and optical properties render them suitable for energy storage, catalysis, and quantum technologies (Montblanch et al., 2023; Raj

et al., 2018; Upadhyay et al., 2021). Molybdenum disulfide (MoS₂), a TMD material, is known for its trigonal prismatic (2H-MoS₂) and octahedral (1T-MoS₂) structures. It has demonstrated remarkable properties for oil and gas applications. For instance, MoS₂ has been used as an alternative catalyst to improve the efficiency of sulfur removal from crude oil (Tuxen et al., 2010). It also exhibits excellent anti-corrosive properties, making it valuable for the oil industry (Aleithan et al., 2023; Joseph et al., 2023; Xia et al., 2019).

Significant studies have shown that MoS₂ nanosheets can alter wettability and improve the oil recovery process (Bhimanapati et al., 2016; Gaur et al., 2014; Kozbial et al., 2015; Luan and Zhou, 2016). Previously, we demonstrated that modified MoS₂ nanosheets possess remarkable oil recovery properties at ultra-low concentrations (Raj et al., 2019). In another study, we stabilized an AOS-based foam using MoS₂ nanosheets and explored its application in foam-based oil recovery (Raj et al., 2020). These modified nanosheets have been successfully injected into various oil reservoirs in China, resulting in a notable reduction in water cut (Qu et al., 2022).

Feng et al. (2022) conducted molecular dynamics simulations to understand the fundamental adsorption behavior of the modified MoS₂ nanosheets at the water/oil interface. They found that IFT is strongly influenced by the competition between the coverage rate of adsorbed nanosheets and the intersection angle arising from non-uniform forces acting on a nanosheet. Zhang et al. (2023) demonstrated that MoS₂ nanosheets modified by organic sulfides can reduce IFT and improve emulsification performance. Although MoS₂ nanosheets can be modified in various ways, achieving an ultra-low IFT and enhancing the stability of the nanofluid under reservoir conditions remains a challenging process. Hence, exploring suitable modification methods to improve the oil displacement-related properties of MoS₂ nanosheets is necessary.

Ethoxylated surfactants are known to contain ethoxy groups (EO), which consist of an oxygen atom connected to two carbon atoms, forming a three-atom chain (White, 1993). This chain is hydrophilic, meaning it has an affinity for water. When introduced into an oil—water system, the EO groups tend to orient themselves towards the water phase (Illous et al., 2020). The hydrophilic EO groups interact with water molecules through hydrogen bonding and other electrostatic interactions, which disrupt the cohesive forces between water molecules and reduce the surface tension at the oil—water interface. As a result, the IFT between the oil and water is lowered. Additionally, the EO groups form a protective layer at the interface, preventing coalescence of oil droplets and maintaining stability in the system through steric stabilization.

Furthermore, incorporating linking units, such as EO groups, between hydrophilic and hydrophobic groups of a surfactant has been shown to significantly enhance interfacial properties and improve salt tolerance (Wang et al., 2015). These surfactants are referred to as extended or ethoxylated surfactants (Miñana-Perez et al., 1995). They exhibit good water hardness tolerance, specific phase behavior, and solubilization performance, and can achieve ultra-low IFT (Wang et al., 2022). Studies have shown that nonionic and anionic surfactants containing EO groups have good salt resistance, excellent resistance to decomposition, and good compatibility (Pal et al., 2019; Priyanto et al., 2022). Sheng et al. (2020) investigated the IFT of fatty alcohol polyoxyethanol carboxylate (C_nEO_mC) mixed solutions against *n*-alkanes, crude oil, and model oils, finding that the best synergism was achieved with a 1:1 mass fraction ratio of C₁₄EO₃C and C₁₄EO₇C. Additionally, Feng et al. (2020) observed that increasing the number of EO groups increases the critical micelle concentration (CMC) of the surfactant. To date, no studies have explored the potential of nanosheet-like materials as extended surfactants. The primary advantage of nanosheets is their ability to function effectively at ultra-low

concentrations, similar to traditional surfactants, due to their high surface area.

In this report, we present the synthesis of ethoxylated MoS₂ nanosheets with a three-dimensional flower-like morphology that exhibits ultra-low IFT and improved stability under oil reservoir conditions. The synthesized material contains an ethoxyl group, which is a polar molecule linked between the MoS₂ nanosheets, and a hydrophobic tail consisting of an alkylamine chain. The presence of the EO group not only increases the tail length but also facilitates a smoother interfacial transition from water to oil. The characterized modified nanosheets were evaluated for their interfacial, emulsion, and oil displacement properties.

2. Experimental

2.1. Materials used

Molybdenum trioxide, thiourea, thioacetamide, and ethanol (99.9% purity) were purchased from Sigma Aldrich, China. *N,N'*-dicyclohexylcarbodiimide (DCC) and trimethylamine (TEA) were purchased from Shanghai Macklin Biochemical Co. Ltd., China. Ethoxylated alkylamine (EO group number: 10—15, carbon number: 12—18) were purchased from RHAWN Chemical Reagent Co., Ltd., Shanghai, China. Lipoic acid (LA) was purchased from Shanghai Aladdin Biochemical Technology Co., Ltd., China.The crude oil with a viscosity of 100 mPa s was obtained from the Jilin Oil Field, China. And the saline water of 40,000 mg/L which represents the conditions of Daqing Oil Field, China was prepared as per Table 1.

2.2. Synthesis of ethoxylated MoS₂ nanosheets

The ethoxylated MoS₂ nanosheets were prepared by subjecting MoS₂ nanosheets to sonication and subsequently reacting them with LA-ethoxylated alkylamine. The complete synthesis process is depicted in Fig. 1.

Initially, MoS_2 nanosheets were synthesized using a simple hydrothermal process according to our previous work (Raj et al., 2019). Briefly, molybdenum trioxide, thioacetamide, and thiourea in a 1:1:10 wt ratio were mixed in 100 mL of deionized water. This mixture was transferred into a 150 mL autoclave and heated at 200 °C for 12 h. After cooling, the precipitated nanosheets were washed with ethanol and deionized water through centrifugation. Finally, the washed MoS_2 nanosheets were freeze-dried and stored for further characterization.

Next, LA was linked with an ethoxylated alkylamine chain following a previous report with some modifications (Feng et al., 2015). One mole equivalent of LA and 2 mol equivalents of ethoxylated alkylamine were combined in 25 mL of ethanol. Subsequently, 50 mg of DCC and 0.15 mL of TEA were added to the mixture, and the resulting solution was stirred for 24 h before being dried to obtain the LA-linked ethoxylated alkylamine chain.

Finally, MoS₂ ethoxylated nanosheets were prepared by grafting the LA-ethoxylated alkylamine group onto the MoS₂ nanosheets through ultrasonication. One weight equivalent of the as-prepared

Table 1
Chemical used and its concentration for preparation of saline water

Chemical	Concentration, mg/L
NaCl	32000
CaCl ₂	6300
MgCl ₂	550
Na ₂ SO ₄	150
NaHCO ₃	1000

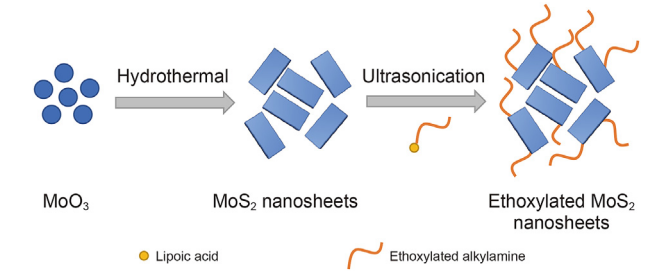


Fig. 1. Schematic illustration of preparation of ethoxylated MoS₂ nanosheets.

LA-linked ethoxylated alkylamine precursor was dispersed with five weight equivalents of MoS_2 nanosheets in deionized water and ultrasonicated for 3 h. The mixture was then stirred for 6 h and dried using a rotary evaporator.

2.3. Preparation of nanofluid

The ethoxylated MoS₂ nanosheets were dispersed in saline water to prepare various concentrations of nanofluid. To prepare the nanofluid without ethoxylate groups, MoS₂ was mixed with 0.01 wt% of octadecylamine (ODA) in ethanol and then ultrasonicated. The resulting product was filtered, dried, and dispersed in saline water for further analysis.

2.4. Characterization

The scanning electron microscope (SEM, FEI Quanta 200F, Thermo Fisher Scientific U.S.A.) and transmission electron microscope (TEM, Technai G2 F20, Thermo Fisher Scientific U.S.A.) were employed to investigate the morphology of the as prepared material. The thickness of the nanosheets was measured using atomic force microscope (AFM, Bruker Mutimode 8, Germany). The structural and crystallographic properties were characterized by Fourier transform infrared spectroscopy (FTIR) and X-ray diffraction (XRD).

2.5. Interfacial analysis

The IFT between the nanofluid and crude oil was measured at 30 °C using the SVT20N spinning drop tensiometer (Dataphysics Corp., Germany) with the following procedure. First, the required concentration of nanofluid was filled into the capillary tube, and then a droplet of crude oil was injected into the center of the tube. The IFT was then measured at a fixed rotational velocity of 6000 rpm at 30 °C and calculated using the following equation.

$$\gamma = 1.2336(r_{\rm W} - r_{\rm o})\omega^2 \left(\frac{D}{n}\right)^3, \quad \frac{L}{D} \ge 4 \tag{1}$$

where γ is oil—nanofluid interfacial surface tension, mN/m; $r_{\rm w}$ is the density of the nanofluid phase, g/cm³; $r_{\rm o}$ is the density of the oil phase, g/cm³; w is the rotational velocity, rpm; D is the measured drop width, mm; L is the length of the oil droplet, mm; and n is the refractive index of the water phase.

2.6. Stability analysis

The TURBISCAN Lab Expert Stabilizer (Formulaction, France) with transmittance light and back-scattering intensity of a pulsed near-infrared light ($\lambda=880$ nm) was used to evaluate the stability of nanofluids. The Zetasizer nano ZS instrument from Malvern Instruments in the United Kingdom was employed to evaluate the

zeta potential of nanofluids, which is also provides the insight of the stability of the nanofluid.

2.7. Emulsion analysis

The prepared nanofluid (10 mL) and hexane dyed with red color (3 mL) were mixed at 3000 rpm for 30 min. The mixture was then left to stabilize for 24 h. Later, a few drops of the emulsion were placed onto a glass substrate and observed using an optical microscope.

2.8. Core flooding analysis

The oil displacement test was carried out at 30 $^{\circ}$ C using core flooding equipment. The overall setup is shown in Fig. 2. The properties of core used to evaluate oil recovery were listed in Table 2.

Initially water was injected into the core sample at an injection rate of 0.3 mL/min and then the respective liquid permeability and porosity of the core sample were calculated. Then the core sample was saturated with crude oil at an injection rate of 0.3 mL/min until no more residual water was produced. Then water flooding was carried out by injecting saline water at an injection rate of 0.3 mL/min until no more oil was produced. Finally, the nanofluid was injected at the same rate until remaining oil was recovery (enhanced or tertiary oil recovery). All the flooding experiments were carried out under the confined pressure of 10 MPa.

3. Results and discussion

3.1. Synthesis of ethoxylated MoS₂ nanosheets

MoS₂ nanosheets were synthesized using a hydrothermal process, as described in the experimental section. Subsequently, lipoic acid, linked with an ethoxylated alkylamine group, was grafted onto the MoS₂ nanosheets. This grafting process utilized a disulfide bridge formed between the sulfur moiety of lipoic acid and the free sulfur present in the defective regions of the MoS₂ nanosheets (Liu et al., 2014). During ultrasonication, the presence of two sulfur atoms in lipoic acid enhances its binding to MoS₂ compared to a single thiol molecule. This enhancement facilitates the strong grafting of the ethoxylated amine group onto the MoS₂ nanosheets.

3.2. Characterization of ethoxylated MoS₂ nanosheets

The sizes and morphologies of the as-prepared materials were characterized using SEM. It revealed a flower-like nanosheet structure, as shown in Fig. 3(a). This structure exposed a large surface area, enabling the adsorption of a greater number of functional groups onto the nanosheet-like material. The lateral size of the as-prepared MoS₂ nanosheets, as depicted in Fig. 3(a), is approximately 75-100 nm. After functionalization of the nanosheets with ethoxy and alkylamine groups, the size remains unchanged, as shown in Fig. 3(b). Further investigation of the microstructure was performed by TEM. Fig. 3(c) shows a TEM image confirming the presence of ultrathin 2D ethoxylated MoS₂ nanosheets. Moreover, the high-resolution TEM (HRTEM) image in Fig. 3(d) reveals a lattice spacing of 0.62 nm which corresponds to the (002) plane of MoS₂. The crystal fringes observed along the curled edge of the (002) plane indicates the formation of layered MoS_2 .

Fig. 4(a) shows the typical tapping mode AFM image and the corresponding height profile of the ethoxylated MoS₂ nanosheets deposited on SiO₂ substrate by spin coating. From its height profile in Fig. 4(b) the measured thickness was found to be approximately

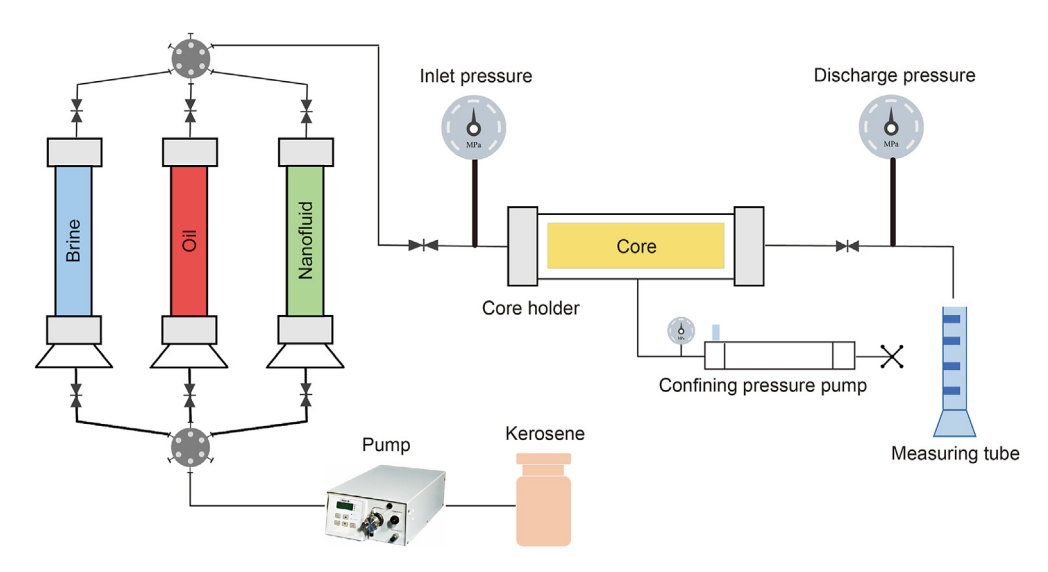


Fig. 2. Core flooding setup.

Table 2 Physical properties of core samples.

Core sample	Diameter, cm	Length, cm	Porosity, %	Permeability, mD
M-2	25.11	108.55	15.7	19.07
M-1	25.24	100.13	15.2	4.99
EM-1	25.02	100.11	15.0	2.66
EM-2	25.18	100.70	15.3	18.3

1.4 nm.

The crystal structures of the as-prepared nanosheets were studied using XRD. Fig. 5(a) shows the XRD patterns of MoS₂ and ethoxylated MoS₂ nanosheets. The XRD peaks at $2\theta=32.9^{\circ}$, 35.7° , 43.3° , and 58.3° correspond to the (100), (102), (006), and (110) peaks of 2H-MoS₂, respectively, as stated on JCPDS card number 37-1492, which agrees with previous reports (Illous et al., 2020; Wang

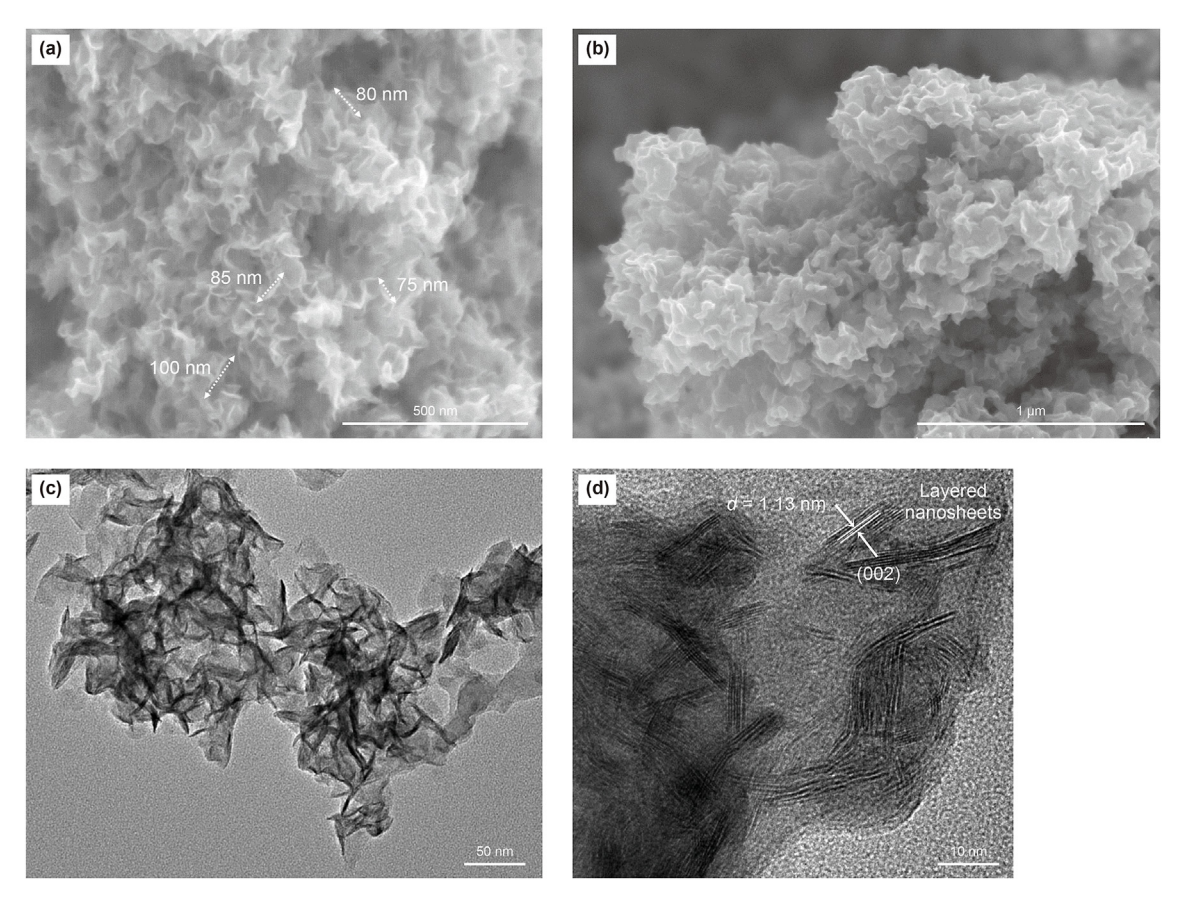


Fig. 3. SEM images of MoS₂ (a) and ethoxylated nanosheets (b); TEM (c) and HRTEM (d) images of ethoxylated nanosheets.

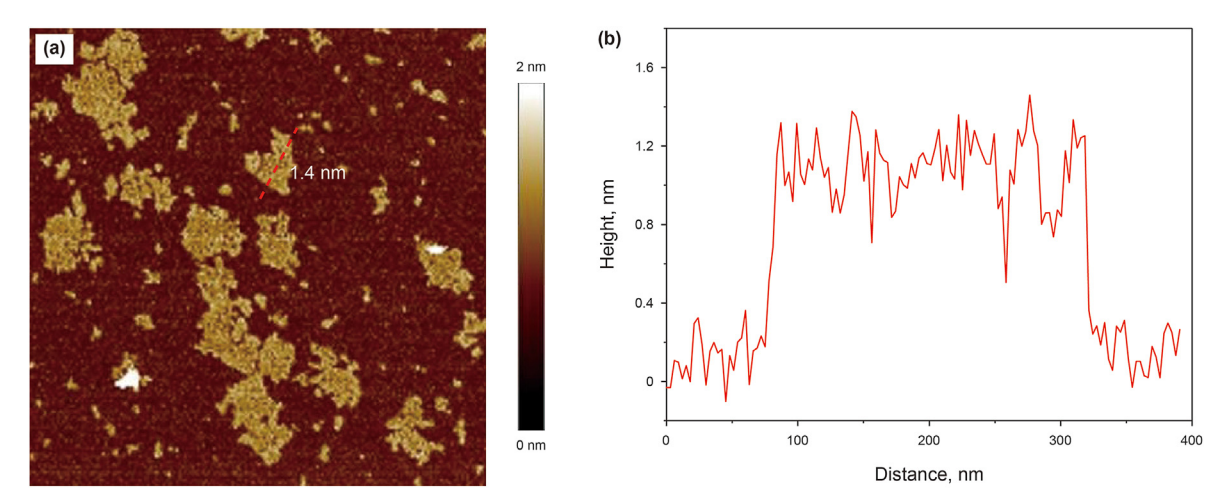


Fig. 4. (a) AFM image of as-synthesized ethoxylated MoS₂ nanosheets and (b) its corresponding height profile.

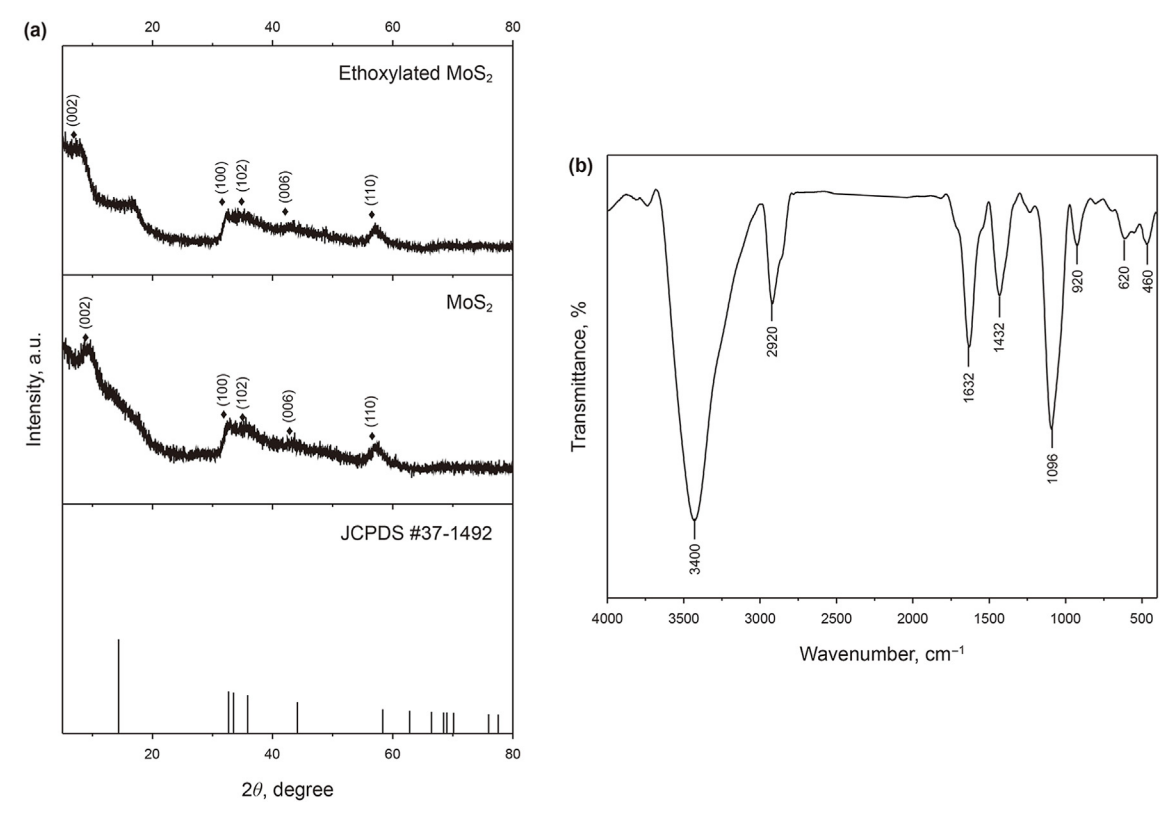


Fig. 5. (a) XRD patterns of ethoxylated MoS₂ and MoS₂ nanosheets; (b) FTIR spectrum of the ethoxylated MoS₂ nanosheets.

et al., 2015). However, due to poor crystallinity caused by the hydrothermal reaction of the as-prepared MoS₂, broader peaks were observed. By comparing the JCPDS card with the synthesized product, we observed a peak shifted from 14.3° to 9.3° for the (002) plane, indicating the presence of the 1T phase of MoS₂. The shift of the (002) plane along the c-axis suggests higher interplanar spacing in 1T-MoS₂ compared to 2H-MoS₂ (Miñana-Perez et al., 1995). The diffraction peak at (002) corresponds to the interlayer spacing (d-spacing = 0.95 nm) of the MoS₂ crystal structure, specifically the distance between sulfur atoms in adjacent layers. After functionalization, the (002) peak shifted from 9.3° to 7.8°, indicating an increase in interlayer spacing. Additionally, the d-spacing for $2\theta = 7.8^\circ$ is found to be 1.13 nm, which agrees well with the HRTEM

image in Fig. 3(d). The broad peaks at 19.5° in the ethoxylated MoS_2 product suggest binding of alkylamine groups to the MoS_2 nanosheets (Illous et al., 2020)

FTIR is used to further confirm the attachment of ethoxylated alkylamine groups onto the nanosheets. Fig. 5(b) shows the FTIR spectrum of the ethoxylated MoS₂ nanosheets, which confirms the presence of both organic and inorganic groups. The presence of MoS₂ is verified by the peaks observed at 920, 620, and 460 cm⁻¹, which correspond to the vibrations of Mo—S, S—H, and out-of-plane vibrations of S atoms, respectively (Raj et al., 2019). The broad peaks between 3700 and 3000 cm⁻¹ and 1632 cm⁻¹ may be the bending vibrations of the O—H in the water molecules adsorbed on the MoS₂ nanosheets (An et al., 2018). The C—H stretching vibration bands

(3000–2800 cm⁻¹) is due to the presence of alkyl chain onto the substance (Yi and Zhang, 2018). Additionally, the peak at 1432 cm⁻¹ originates from the C–N stretching of the amide group. The presence of a peak at 1096 cm⁻¹ is attributed to the stretching vibration of the C–O bond in the ethoxy group (Priyanto et al., 2022). Therefore, the FTIR spectrum confirms the presence of the ethoxy and alkylamine chains onto the MoS₂ nanosheets.

3.3. Interfacial properties

The fluid interfacial behaviour plays the major role in EOR as it diminishes the adhesion of residual oil within pore structures, thereby enhancing oil displacement by increasing the capillary number (Bashir et al., 2022). In conventional surfactants, the spacer extends the hydrophobic tail and facilitates a seamless interfacial transition between aqueous and oleic phases. In this study, ethylene oxide acts as a spacer or intermediate group, linking the alkylamine tail to MoS_2 nanosheets, which act as the hydrophilic head group. This configuration significantly enhances the interfacial properties of the ethoxylated MoS_2 nanosheets.

Fig. 6 illustrates the IFT between oil and nanofluids under various conditions. The concentration of MoS_2 nanosheets dispersed over the ethoxylated alkylamine chain was optimized based on their interfacial performance. Fig. 6(a) shows the IFT behavior at varying MoS_2 concentrations with ethoxylated alkylamine chains, achieving a minimum IFT of 0.008 mN/m at 50 ppm. However, above 100 ppm, poor dispersion of MoS_2 in water leads to

aggregation and precipitation, reducing nanosheet spacing due to cohesive forces between molecules. As a result, the van der Waals force dominates over the repulsive force between the molecules, which increases the surface tension (Israelachvili, 1974). Another reason contributing to the increase in IFT is the self-adsorption of molecules at surfaces to minimize surface energy and surface tension (De Aguiar et al., 2011). Initially, surface tension decreases significantly with increasing surfactant concentration but rises once the critical micelle concentration (CMC) is surpassed. The CMC is the minimum concentration at which surfactants aggregate into micelles in an oil-water system. Below 100 mg/L nanofluid concentration, there is adequate interfacial area for nanosheet selfadsorption, sharply reducing IFT. Above CMC, excess surfactant molecules form micelle aggregates, offering no further IFT improvement, Fig. 6(b) demonstrates achieving the lowest IFT of approximately 0.005 mN/m at 50 ppm concentration.

Compared to traditional surfactants, the synthesized nanofluid exhibits a significantly lower CMC due to the higher density of surface-active sites on MoS₂ nanosheets (Xie et al., 2013). These surface-active sites enhance the binding capacity of the ethoxylated alkylamine chains. Hence, a single MoS₂ nanosheet can bind more hydrophilic chains, facilitating the attainment of CMC at ultra-low concentrations.

Fig. 6(c)and (d) depict images of an oil—nanofluid system obtained using a spinning drop tensiometer, showcasing the system with and without the presence of EO groups on the nanosheets, respectively. The spinning drop tensiometer operates by rotating a

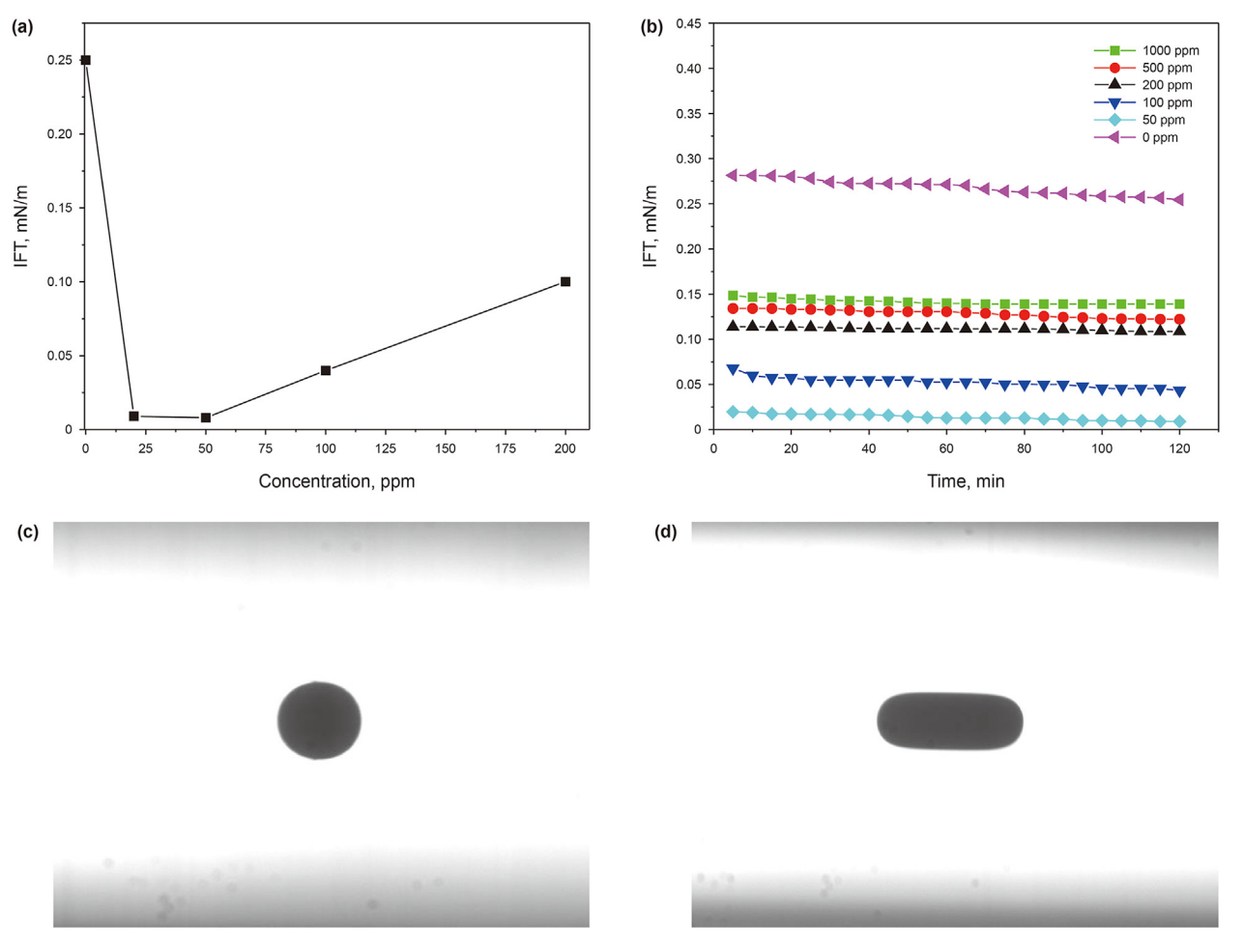


Fig. 6. (a) IFT of various MoS₂ concentrations against the ethoxylated alkylamine chains; (b) IFT of the nanofluids at various concentrations of ethoxylated MoS₂; (c) and (d) represent the images of the oil—nanofluid system taken from a spinning drop tensiometer with and without the presence of EO groups over the nanosheets, respectively.

horizontal tube, generating a centrifugal force that elongates the oil drop until the IFT balances the centrifugal forces. The extent of the oil drop's elongation is inversely related to the IFT between the two liquids, with a lower IFT resulting in a more elongated shape. From Fig. 6(c) and (d), a noticeable difference in the size and shape of cylindrical oil droplets is observed. The droplet in the presence of EO groups is more elongated compared to the droplet without EO groups, indicating a lower IFT when EO groups are present. Adding EO groups to the hydrophilic MoS₂ nanosheets enhances their interaction with water molecules, thereby weakening the interaction between the hydrophobic alkylamine groups on the nanosheets and the oil. This results in an energy imbalance between these interactions. Consequently, the presence of EO groups reduces the interaction of the nanofluid at the oil-water interface, lowering the IFT and leading to a more elongated oil drop. This behaviour demonstrates the significant effect of EO groups on the interfacial properties of the nanofluid system.

3.4. Stability of the nanofluid

The presence of EO groups over the MoS₂ nanosheets enhances their stability in water. The stability evaluation of functionalization of nanosheets with and without EO groups was assessed by visual observation and multiple-light scattering using the Turbiscan (Fig. 7). Fig. 7(a) displays bottles containing nanofluids with (E-MoS₂) and without (MoS₂) EO groups at various time intervals, with the nanofluid concentration of 50 ppm. It was observed that the

nanofluid without EO groups became translucent and the nanosheets settled at the bottom after 24 h. In contrast, the nanofluid containing the EO groups remained stable with only slight changes in stability observed after 24 h. To further investigate the instability of the nanofluid suspension at room temperature, multiple-light scattering was employed. The transmission spectrum of E-MoS₂ shown in Fig. 7(b), with the x-axis representing the height of the nanofluid and the y-axis representing the transmission light intensity (T). Different colors in the spectrum represent the scanning at different time intervals.

The sedimentation of MoS_2 nanosheets typically occurs to a height of less than 2 mm on the sample holder. Consequently, we observe an increase in transmission intensity at a height of 2 mm for both nanofluids. The clarification process occurs above 2 mm on the sample holder. Additionally, a destabilized spectrum is observed on the clarification regime, which is due to the agglomeration of the nanosheets.

The Turbiscan stability index (TSI) is relates the variation of transmittance and back scattering light intensities with respect to the initial ones. It evaluates the stability of the nanofluid.

$$TSI = \sum_{i} \frac{\sum_{h} |scan_{i}(h) - scan_{i-1}(h)|}{H}$$
 (2)

where i is the number of scanning; h is the height of the scanning point; $scan_i(h)$ is the average light intensity; H is the height of the

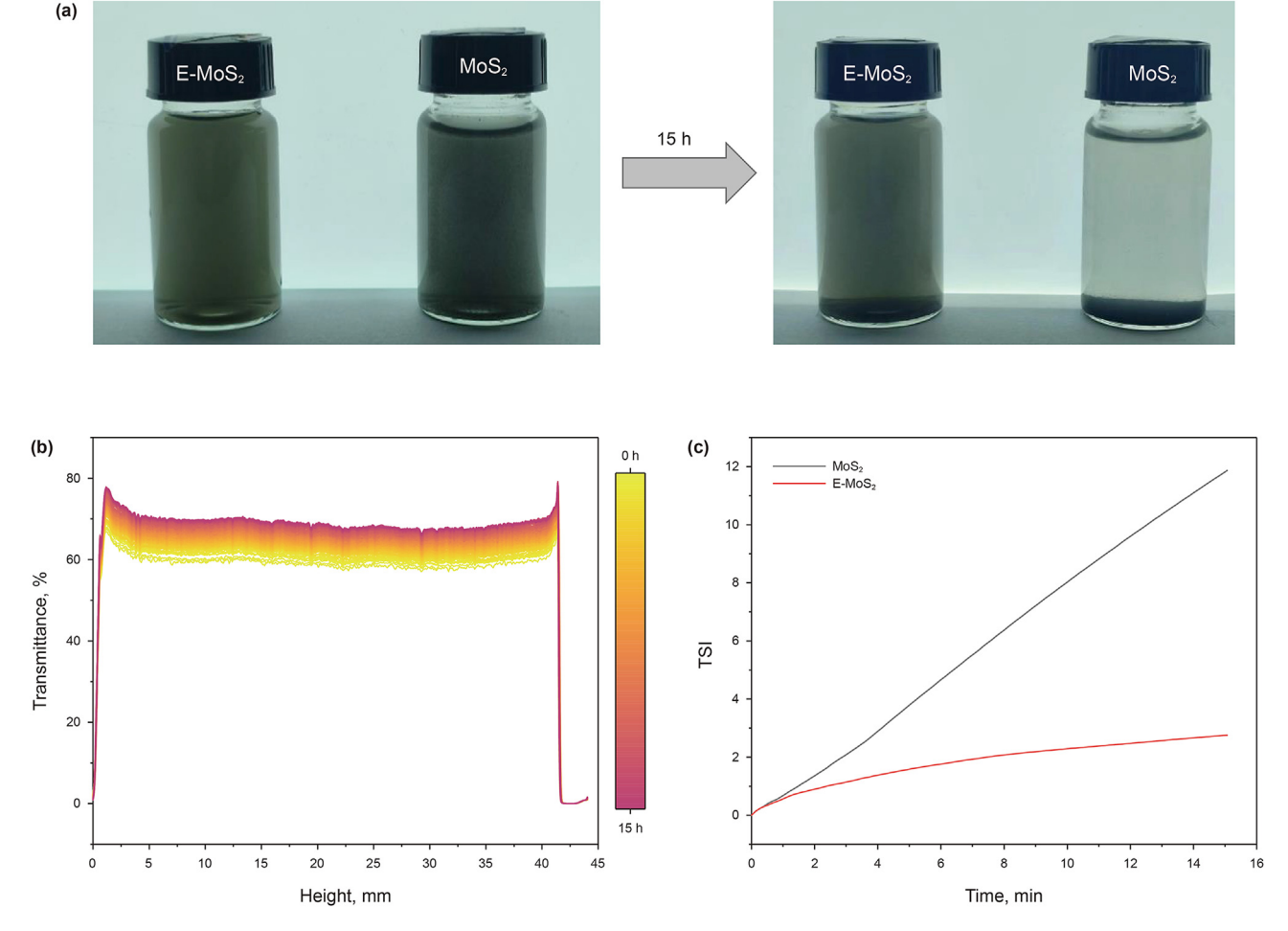


Fig. 7. (a) Images of bottles containing nanofluids with (E-MoS₂) and without (MoS₂) EO groups; (b) Transmission spectrum of E-MoS₂; (c) TSI curves of E-MoS₂ and MoS₂ nanofluids.

sample.

The higher the TSI value, the less stable the nanofluid. The lower the TSI value, the more stable the nanofluid (Hutin and Carvalho, 2022). The TSI curve in Fig. 7(c) shows this relationship as it pertains to the presence or absence of EO groups in the nanofluid. It is evident from the TSI curve that the nanofluid with EO groups is more stable compared to the nanofluid without EO groups. This enhanced stability is attributed to the EO groups on the nanosheets, which promote strong hydrophilicity and interaction with water molecules. As a result, the nanosheets with EO groups primarily remain dispersed in the water phase and exhibit outward extension, enhancing overall stability of the nanofluid.

Zeta potential is another crucial measure for assessing the stability of nanofluids. Higher stability is typically associated with a higher absolute value of zeta potential. Stable dispersions generally require a zeta potential of ± 30 mV or greater (Pandey et al., 2024). From Fig. 8, it can be inferred that the zeta potential of the MoS2 nanofluid is generally -12 mV, but when EO groups are added, it increases to -38 mV. This increase in zeta potential in the nanofluid with EO groups is attributed to the enhanced electrostatic repulsion between particles facilitated by EO groups. This repulsion mechanism effectively prevents particle aggregation or flocculation, thereby contributing to a more stable nanofluid.

3.5. Emulsification property

Enhancing the emulsion stability is a critical parameter to improve the effectiveness of the enhanced oil recovery process. Several studies have reported that amphiphilic nanomaterials can stabilize emulsions. In this study, we investigated emulsion stability by mixing heptane and nanofluid, then emulsifying the mixture using an ultrasonic oscillator. After allowing the mixture to settle for 24 h, we observed the stabilized emulsified droplets using an optical microscope (Fig. 9). To compare, we also analysed the emulsion droplets of nanofluid containing MoS₂ nanosheets with and without EO groups. It was observed that the emulsion stability of the nanofluid with EO groups was more stable than the other. The emulsion observed was in the form of dispersed oil droplets, indicating that it was an oil-in-water emulsion. Furthermore, Fig. 9(a) shows that nanosheets tend to settle at the interface of oil and water due to their amphiphilic nature. In contrast, Fig. 9(b)

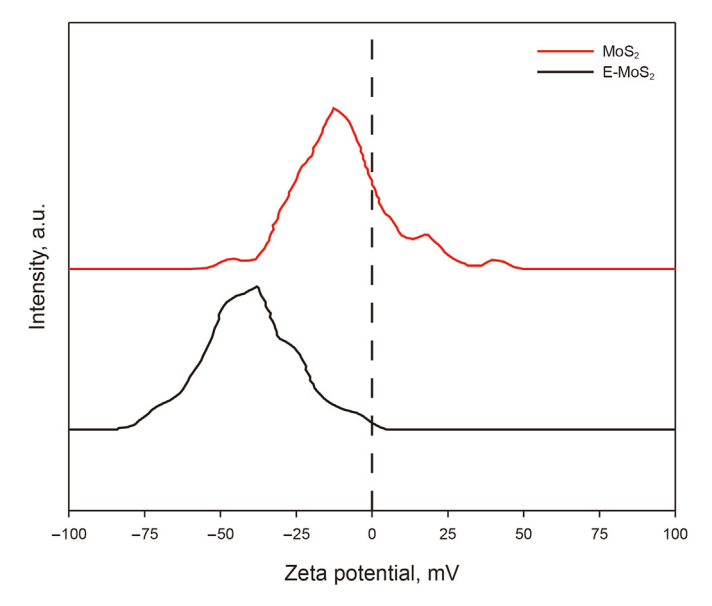


Fig. 8. Zeta potential of the nanofluids with (E-MoS₂) and without (MoS₂) EO groups.

illustrates that the emulsified oil droplets benefit from the interaction of hydrophilic EO groups with water molecules and hydrophobic alkylamine chains with oil molecules. This interaction facilitates the formation of a monolayer at the interface, which acts as a protective coating around the oil droplets. This monolayer prevents coalescence and merging of oil droplets, reducing the IFT between the oil and water phases (Grigoriev and Miller, 2009). As a result, the emulsion is easier to form and remains more stable. Additionally, the addition of EO groups makes the emulsion more resistant to coalescence, as more nanosheets accumulate at the oil—water interface, increasing electrostatic repulsion between the oil droplets. This enhances stability by reducing the polarity difference between hydrophilic and hydrophobic groups, leading to longer-lasting interactions at the oil—water interface and the formation of micro-emulsions.

3.6. Oil recovery studies

The sand pack flooding experiment was conducted to evaluate the effectiveness of the prepared nanofluid for enhanced oil recovery. The method used in the experiment is detailed in Section 2.8. The nanofluid containing MoS₂ with an alkylamine chain was tested in core plugs M1 and M2, while the nanofluid with ethoxylated MoS2 nanosheets was tested in core plugs EM1 and EM2. All core plugs had a porosity of approximately 15%. The recovery factor was calculated by dividing the cumulative oil produced by the known initial oil in place and expressed as a percentage. The average recovery rate by water flooding was found to be 45%. After brine injection, the nanofluid was injected for a total of 7-8 pore volume (PV). Fig. 10 shows the plot of the oil recovery rate as a function of injection volume. Our observations reveal that the ethoxylated nanofluid is more effective in producing oil than the nanofluid with only alkylamine groups. This is mainly because of the presence of EO groups between the MoS2 nanosheets and the hydrophobic alkylamine chain, which weakens the interaction between the hydrophobic alkylamine group and the oil, and also lowers the interaction of the nanofluid at the interface, thereby reducing the IFT value to approximately 10^{-3} mN/m at concentrations less than about 50 ppm. Additionally, the formation of oil-in-water micro emulsions is another reason for enhanced oil recovery with the nanofluid containing EO groups. We also observed that the oil recovery rate is higher in low-permeability core plugs compared to higher permeability ones. This is due to the increased specific surface area of low-permeability cores, which extends the contact time of oil with the nanosheets, resulting in more oil being desorbed from the pores (Qu et al., 2021). The pressure gauge with a range of 0-24 bar was utilized to measure the differential pressure. After the initial brine solution injection, the oil recovery led to a significant drop in pressure. Once water breakthrough occurred, the pressure levels stabilized. Finally, the recovery of the residual oil leads to a decrease in the differential pressure.

4. Conclusions

In conclusion, we have demonstrated a new approach to synthesis the extended surfactants like nanomaterials, for EOR. Our synthesized nanomaterial features an ethoxy group linking MoS_2 nanosheets with a hydrophobic alkylamine tail. We observed that the prepared nanofluid exhibits an ultra-low interfacial tension of approximately 10^{-3} mN/m and remains stable under oil reservoir conditions at a low concentration of 50 ppm. Additionally, we observed the formation of stable oil-in-water microemulsions, which ultimately led to an increased oil recovery rate at low permeable core plugs. Therefore, the synthesized ethoxylated

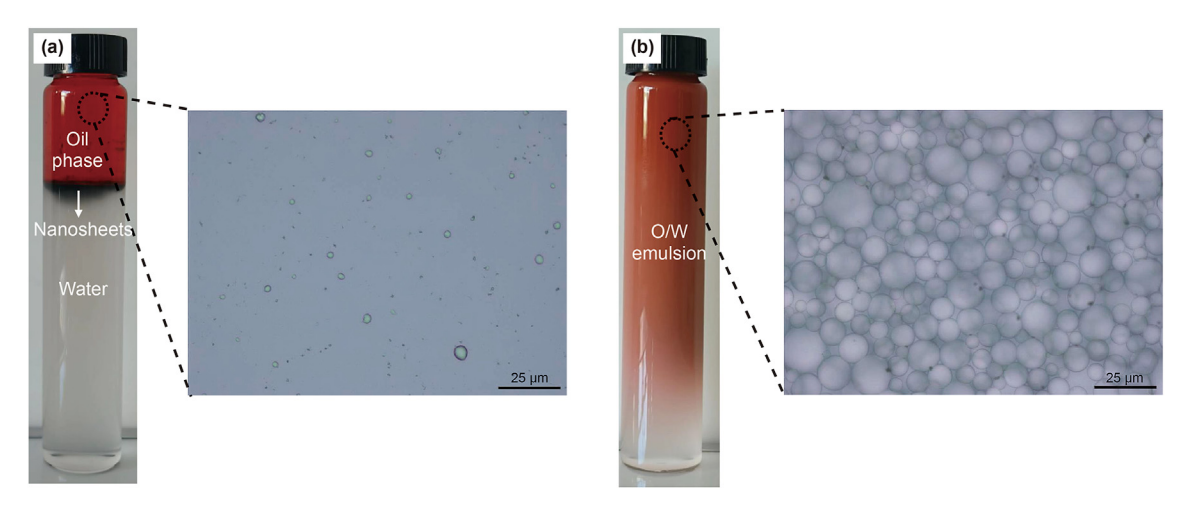


Fig. 9. Photographic and optical microscopic images of emulsified oil/nanofluids without (a) and with (b) EO groups.

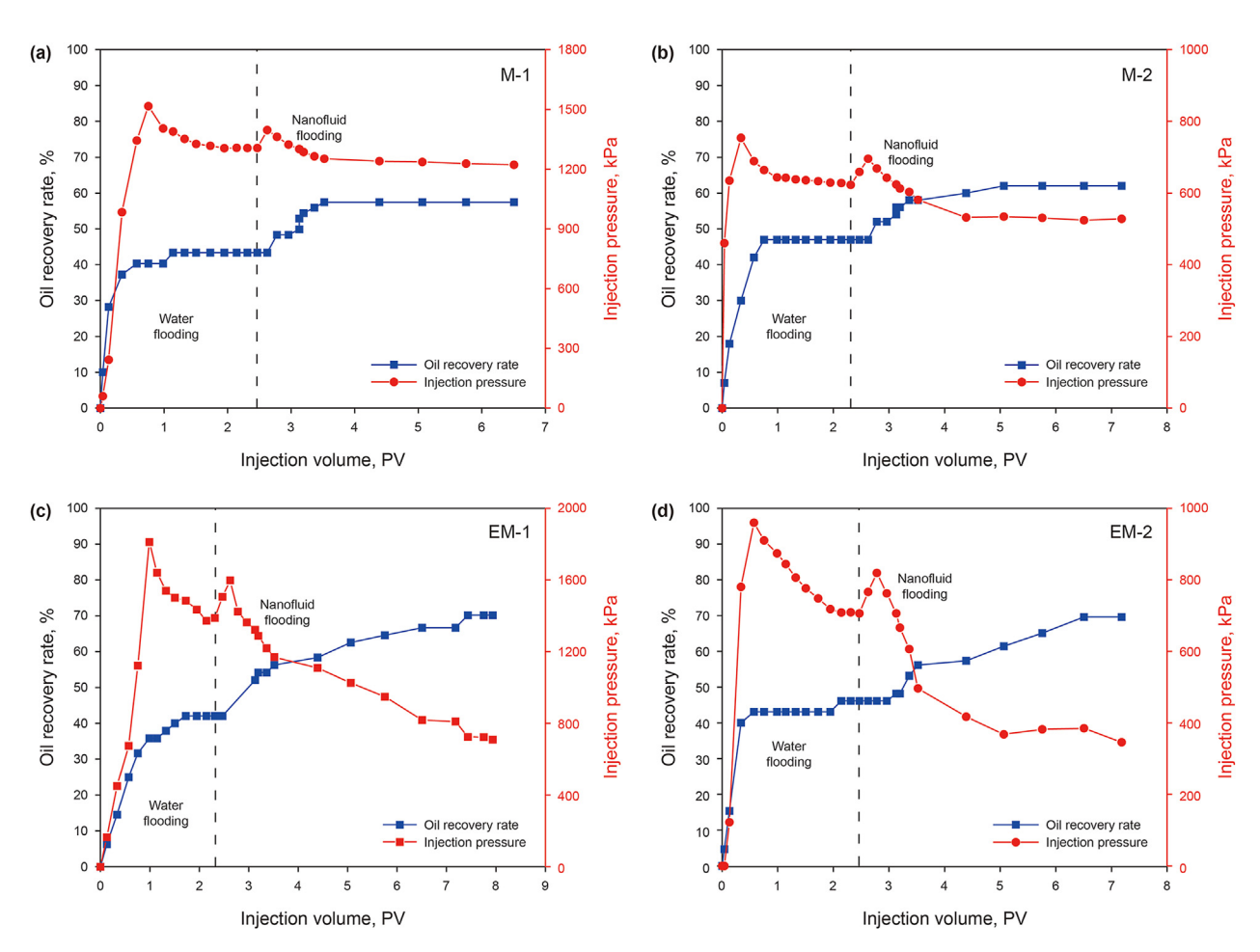


Fig. 10. Oil recovery and pressure drop performance of the nanofluids for core plugs M1 (a), M2 (b), EM1 (c), and EM2 (d).

nanosheets are an excellent candidate for chemical EOR in low-permeability reservoirs. Further research can be conducted on controlling the IFT by manipulating the number of ethoxy groups.

CRediT authorship contribution statement

Infant Raj: Writing – review & editing, Writing – original draft, Visualization, Validation, Supervision, Project administration,

Methodology, Investigation, Formal analysis, Data curation, Conceptualization. **Zhuo Lu:** Resources, Formal analysis. **Ji-Rui Hou:** Investigation, Funding acquisition. **Yu-Chen Wen:** Visualization. **Li-Xiao Xiao:** Visualization, Validation.

Declaration of competing interest

The authors declare that they have no known competing

financial interests or personal relationships that could have appeared to influence the work reported in this paper.

Acknowledgement

This work has been funded by the National Natural Science Foundation of China (No. 52174046).

References

- Ahmadi, A., Manshad, A.K., Akbari, M., Ali, J.A., Jaf, P.T., Abdulrahman, A.F., 2024. Nano-stabilized foam for enhanced oil recovery using green nanocomposites and anionic surfactants: an experimental study. Energy 290, 130201. https:// doi.org/10.1016/j.energy.2023.130201.
- Aleithan, S.H., Al-Amer, K., Alabbad, Z.H., Khalaf, M.M., Alam, K., Alhashem, Z., El-Lateef, H.M.A., 2023. Highly scalable synthesis of MoS₂ thin films for carbon steel coatings: influence of synthetic route on the nanostructure and corrosion performance. J. Mater. Res. Technol. 23, 1239–1251. https://doi.org/10.1016/j.jmrt.2023.01.048.
- An, J., Wang, X., Ming, M., Li, J., Ye, N., 2018. Determination of sulfonamides in milk by capillary electrophoresis with PEG@MoS₂ as a dispersive solid-phase extraction sorbent. R. Soc. Open Sci. 5 (5), 172104. https://doi.org/10.1098/ rsos.172104.
- Bashir, A., Haddad, A.S., Rafati, R., 2022. A review of fluid displacement mechanisms in surfactant-based chemical enhanced oil recovery processes: analyses of key influencing factors. Petrol. Sci. 19 (3), 1211–1235. https://doi.org/10.1016/ i.petsci.2021.11.021.
- Bhimanapati, G.R., Hankins, T., Lei, Y., Vilá, R.A., Fuller, I., Terrones, M., Robinson, J.A., 2016. Growth and tunable surface wettability of vertical MoS₂ layers for improved hydrogen evolution reactions. ACS Appl. Mater. Interfaces 8 (34), 22190–22195. https://doi.org/10.1021/acsami.6b05848.
- Chowdhury, T., Sadler, E.C., Kempa, T.J., 2020. Progress and prospects in transition-metal dichalcogenide research beyond 2D. Chem. Rev. 120 (22), 12563—12591. https://doi.org/10.1021/acs.chemrev.0c00505.
- De Aguiar, H.B., Strader, M.L., de Beer, A.G., Roke, S., 2011. Surface structure of sodium dodecyl sulfate surfactant and oil at the oil-in-water droplet liquid/liquid interface: a manifestation of a nonequilibrium surface state. J. Phys. Chem. B 115 (12), 2970–2978. https://doi.org/10.1021/jp200536k.
- Deng, X., Tariq, Z., Murtaza, M., Patil, S., Mahmoud, M., Kamal, M.S., 2021. Relative contribution of wettability alteration and interfacial tension reduction in EOR: a critical review. J. Mol. Liq. 325, 115175. https://doi.org/10.1016/j.molliq.2020.115175.
- Desai, S.B., Madhvapathy, S.R., Sachid, A.B., Llinas, J.P., Wang, Q., Ahn, G.H., Pitner, G., Kim, M.J., Bokor, J., Hu, C., 2016. MoS₂ transistors with 1-nanometer gate lengths. Science 354 (6308), 99–102. https://doi.org/10.1126/science.aah4698.
- Eltoum, H., Yang, Y.-L., Hou, J.-R., 2021. The effect of nanoparticles on reservoir wettability alteration: a critical review. Petrol. Sci. 18, 136–153. https://doi.org/10.1007/s12182-020-00496-0.
- Feng, N., Zhao, T., Zhao, Y., Song, P., Li, G., Zhang, G., 2020. Adsorption and aggregation behavior of aliphatic alcohol polyoxyethylene ether phosphate with different ethylene oxide addition numbers. Colloids Surf. A Physicochem. Eng. Asp. 586, 124215. https://doi.org/10.1016/j.colsurfa.2019.124215.
- Feng, W., Chen, L., Qin, M., Zhou, X., Zhang, Q., Miao, Y., Qiu, K., Zhang, Y., He, C., 2015. Flower-like PEGylated MoS₂ nanoflakes for near-infrared photothermal cancer therapy. Sci. Rep. 5 (1), 17422. https://doi.org/10.1038/srep17422.
- Feng, Y., Hou, J., Yang, Y., Wang, S., Wang, D., Cheng, T., You, Z., 2022. Morphology of MoS₂ nanosheets and its influence on water/oil interfacial tension: a molecular dynamics study. Fuel 312, 122938. https://doi.org/10.1016/j.fuel.2021.122938.
- Gaur, A.P., Sahoo, S., Ahmadi, M., Dash, S.P., Guinel, M.J.-F., Katiyar, R.S., 2014. Surface energy engineering for tunable wettability through controlled synthesis of MoS₂. Nano Lett. 14 (8), 4314–4321. https://doi.org/10.1021/nl501106v.
- Grigoriev, D.O., Miller, R., 2009. Mono-and multilayer covered drops as carriers.

 Curr. Opin. Colloid Interface Sci. 14 (1), 48–59. https://doi.org/10.1016/
- Halari, D., Yadav, S., Kesarwani, H., Saxena, A., Sharma, S., 2024. Nanoparticle and surfactant stabilized carbonated water induced in-situ CO₂ foam: an improved oil recovery approach. Energy & Fuels. https://doi.org/10.1021/acs.energyfuels.3c04232.
- Hutin, A., Carvalho, M.S., 2022. Effect of contamination from direct sonication on characterization of nanofluid stability. Powder Technol. 399, 117157. https:// doi.org/10.1016/j.powtec.2022.117157.
- Illous, E., Ontiveros, J.F., Lemahieu, G., Lebeuf, R., Aubry, J.-M., 2020. Amphiphilicity and salt-tolerance of ethoxylated and propoxylated anionic surfactants. Colloids Surf. A Physicochem. Eng. Asp. 601, 124786. https://doi.org/10.1016/ j.colsurfa.2020.124786.
- Israelachvili, J.N., 1974. The nature of van der Waals forces. Contemp. Phys. 15 (2), 159–178. https://doi.org/10.1080/00107517408210785. Jiang, D., Liu, Z., Xiao, Z., Qian, Z., Sun, Y., Zeng, Z., Wang, R., 2022. Flexible elec-
- Jiang, D., Liu, Z., Xiao, Z., Qian, Z., Sun, Y., Zeng, Z., Wang, R., 2022. Flexible electronics based on 2D transition metal dichalcogenides. J. Mater Chem. A 10 (1), 89–121. https://doi.org/10.1039/D1TA06741A.
- Joseph, A., Vijayan, A.S., Shebeeb, C.M., Akshay, K.S., Mathew, K.J.P., Sajith, V., 2023. A review on tailoring the corrosion and oxidation properties of MoS₂-based

coatings. J. Mater Chem. A 11 (7), 3172–3209. https://doi.org/10.1039/d2ta07821i

- Kazemzadeh, Y., Shojaei, S., Riazi, M., Sharifi, M., 2019. Review on application of nanoparticles for EOR purposes: a critical review of the opportunities and challenges. Chin. J. Chem. Eng. 27 (2), 237–246. https://doi.org/10.1016/ j.cjche.2018.05.022.
- Kesarwani, H., Khan, F., Tandon, A., Azin, R., Osfouri, S., Sharma, S., 2022a. Performance improvement of the surfactant polymer flooding using bio synthesized calcium carbonate nanoparticles: an experimental approach. Arabian J. Sci. Eng. 47 (9), 11775–11792. https://doi.org/10.1007/s13369-022-06571-5.
- Kesarwani, H., Srivastava, V., Mandal, A., Sharma, S., Choubey, A.K., 2022b. Application of α-MnO₂ nanoparticles for residual oil mobilization through surfactant polymer flooding. Environ. Sci. Pollut. Control Ser. 29 (29), 44255–44270. https://doi.org/10.1007/s11356-022-19009-0.
- Kozbial, A., Gong, X., Liu, H., Li, L., 2015. Understanding the intrinsic water wettability of molybdenum disulfide (MoS₂). Langmuir 31 (30), 8429–8435. https:// doi.org/10.1021/acs.langmuir.5b02057.
- Liu, T., Wang, C., Gu, X., Gong, H., Cheng, L., Shi, X., Feng, L., Sun, B., Liu, Z., 2014. Drug delivery with PEGylated MoS₂ nano-sheets for combined photothermal and chemotherapy of cancer. Advanced Materials (Deerfield Beach, Fla.) 26 (21), 3433–3440. https://doi.org/10.1002/adma.201305256.
- Luan, B., Zhou, R., 2016. Wettability and friction of water on a MoS₂ nanosheet. Appl. Phys. Lett. 108 (13) https://doi.org/10.1063/1.4944840
- Phys. Lett. 108 (13). https://doi.org/10.1063/1.4944840.

 Mackin, C., Fasoli, A., Xue, M., Lin, Y., Adebiyi, A., Bozano, L., Palacios, T., 2020. Chemical sensor systems based on 2D and thin film materials. 2D Mater. 7 (2), 022002. https://doi.org/10.1088/2053-1583/ab6e88.
- Manshad, A.K., Mobaraki, M., Ali, J.A., Akbari, M., Abdulrahman, A.F., Jaf, P.T., Bahraminejad, H., Sajadi, S.M., 2024. Performance evaluation of the green surfactant-treated nanofluid in enhanced oil recovery: dill-hop extracts and SiO₂/bentonite nanocomposites. Energy & Fuels 38 (3), 1799–1812. https://doi.org/10.1021/acs.energyfuels.3c04335.
- Miñana-Perez, M., Graciaa, A., Lachaise, J., Salager, J.-L., 1995. Solubilization of polar oils with extended surfactants. Colloids Surf. A Physicochem. Eng. Asp. 100, 217–224. https://doi.org/10.1016/0927-7757(95)03186-H.
- Mirzavandi, M., Ali, J.A., Manshad, A.K., Majeed, B., Mahmood, B.S., Mohammadi, A.H., Iglauer, S., Keshavarz, A., 2023. Performance evaluation of silica-graphene quantum dots for enhanced oil recovery from carbonate reservoirs. Energy & Fuels 37 (2), 955–964. https://doi.org/10.1021/acs.energyfuels.2c03150.
- Montblanch, A.R.-P., Barbone, M., Aharonovich, I., Atatüre, M., Ferrari, A.C., 2023. Layered materials as a platform for quantum technologies. Nat. Nanotechnol. 1–17. https://doi.org/10.1038/s41565-023-01354-x.
- Motraghi, F., Manshad, A.K., Akbari, M., Ali, J.A., Sajadi, S.M., Iglauer, S., Keshavarz, A., 2023. Interfacial tension reduction of hybrid crude-oil/mutual-solvent systems under the influence of water salinity, temperature and green SiO₂/KCl/xanthan nanocomposites. Fuel 340, 127464. https://doi.org/10.1016/j.fuel.2023.127464.
- Pal, N., Samanta, K., Mandal, A., 2019. A novel family of non-ionic gemini surfactants derived from sunflower oil: synthesis, characterization and physicochemical evaluation. J. Mol. Liq. 275, 638–653. https://doi.org/10.1016/ j.molliq.2018.11.111.
- Pandey, A., Roy, V., Kesarwani, H., Sharma, S., Saxena, A., 2022. Evaluation of silicon carbide nanoparticles as an additive to minimize surfactant loss during chemical flooding. ChemistrySelect 7 (22), e202104294. https://doi.org/ 10.1002/slct.202104294.
- Pandey, A., Kesarwani, H., Tewari, C., Saxena, A., Sharma, S., Sahoo, N.G., 2023. Waste plastic derived reduced graphene oxide as a potential additive for the surfactant polymer flooding: a sustainable solution. J. Environ. Chem. Eng. 11 (3), 109661. https://doi.org/10.1016/j.jece.2023.109661.
- Pandey, A., Qamar, S.F., Das, S., Basu, S., Kesarwani, H., Saxena, A., Sharma, S., Sarkar, J., 2024. Advanced multi-wall carbon nanotube-optimized surfactant-polymer flooding for enhanced oil recovery. Fuel 355, 129463. https://doi.org/10.1016/j.fuel.2023.129463.
- Priyanto, S., Sudrajat, R.W., Suherman, S., Pramudono, B., Riyanto, T., Dasilva, T.M., Yuniar, R.C., Aviana, H., 2022. High-performance polymeric surfactant of sodium lignosulfonate-polyethylene glycol 4000 (SLS-PEG) for enhanced oil recovery (EOR) process. Periodica Polytechnica Chemical Engineering 66 (1), 114–124. https://doi.org/10.3311/PPch.17972.
- Qu, M., Hou, J., Liang, T., Qi, P., 2021. Amphiphilic rhamnolipid molybdenum disulfide nanosheets for oil recovery. ACS Appl. Nano Mater. 4 (3), 2963–2972. https://doi.org/10.1021/acsanm.1c00102.
- Qu, M., Liang, T., Hou, J., Liu, Z., Yang, E., Liu, X., 2022. Laboratory study and field application of amphiphilic molybdenum disulfide nanosheets for enhanced oil recovery. J. Petrol. Sci. Eng. 208, 109695. https://doi.org/10.1016/ i.petrol.2021.109695.
- Raj, I., Duan, Y., Kigen, D., Yang, W., Hou, L., Yang, F., Li, Y., 2018. Catalytically enhanced thin and uniform TaS₂ nanosheets for hydrogen evolution reaction. Front. Mater. Sci. 12, 239–246. https://doi.org/10.1007/s11706-018-0425-0.
- Raj, I., Liang, T., Qu, M., Xiao, L., Hou, J., Xian, C., 2020. An experimental investigation of MoS₂ nanosheets stabilized foams for enhanced oil recovery application. Colloids Surf. A Physicochem. Eng. Asp. 606, 125420. https://doi.org/10.1016/ j.colsurfa.2020.125420.
- Raj, I., Qu, M., Xiao, L., Hou, J., Li, Y., Liang, T., Yang, T., Zhao, M., 2019. Ultralow concentration of molybdenum disulfide nanosheets for enhanced oil recovery. Fuel 251, 514–522. https://doi.org/10.1016/j.fuel.2019.04.078.
- Sheng, S.-S., Cao, X.-L., Zhu, Y.-W., Jin, Z.-Q., Zhang, L., Zhu, Y., Zhang, L., 2020.

- Structure-activity relationship of anionic-nonionic surfactant for reducing interfacial tension of crude oil. J. Mol. Liq. 313, 112772. https://doi.org/10.1016/impollig.2020.112772
- Tan, T., Jiang, X., Wang, C., Yao, B., Zhang, H., 2020. 2D material optoelectronics for information functional device applications: status and challenges. Adv. Sci. 7 (11), 2000058. https://doi.org/10.1002/advs.202000058.
- Tuxen, A., Kibsgaard, J., Gobel, H., Laegsgaard, E., Topsoe, H., Lauritsen, J.V., Besenbacher, F., 2010. Size threshold in the dibenzothiophene adsorption on MoS₂ nanoclusters. ACS Nano 4 (8), 4677–4682. https://doi.org/10.1021/ nn1011013.
- Upadhyay, S.N., Satrughna, J.A.K., Pakhira, S., 2021. Recent advancements of two-dimensional transition metal dichalcogenides and their applications in electrocatalysis and energy storage. Emergent Materials 4 (4), 951–970. https://doi.org/10.1007/s42247-021-00241-2.
- Vats, S., Khan, F., Prajapati, D., Pandey, A., Sharma, S., Saxena, A., 2023. Synthesis and evaluation of mesoporous silica nanoparticle and its application in chemical enhanced oil recovery. ChemistrySelect 8 (12), e202204206. https://doi.org/10.1002/slct.202204206.
- Wang, C., Fang, S., Duan, M., Xiong, Y., Ma, Y., Chen, W., 2015. Synthesis and evaluation of demulsifiers with polyethyleneimine as accepter for treating crude oil emulsions. Polym. Adv. Technol. 26 (5), 442–448. https://doi.org/10.1002/pat/3471
- Wang, Z.-S., Zhou, Z.-H., Han, L., Chen, X., He, H.-J., Zhang, O., Xu, Z.-C., Gong, O.-T.,

- Zhang, L., Ma, G.-Y., 2022. The mechanism for lowering interfacial tension by extended surfactant containing ethylene oxide and propylene oxide groups. J. Mol. Liq. 359, 119364. https://doi.org/10.1016/j.molliq.2022.119364.
- White, G.F., 1993. Bacterial biodegradation of ethoxylated surfactants. Pestic. Sci. 37 (2), 159–166. https://doi.org/10.1002/ps.2780370209.
- Xia, Y.Q., He, Y., Chen, C.L., Wu, Y.Q., Chen, J.Y., 2019. MoS₂ nanosheets modified SiO₂ to enhance the anticorrosive and mechanical performance of epoxy coating. Prog. Org. Coat 132, 316–327. https://doi.org/10.1016/j.porgcoat.2019.04.002.
- Xie, J., Zhang, H., Li, S., Wang, R., Sun, X., Zhou, M., Zhou, J., Lou, X.W., Xie, Y., 2013. Defect-rich MoS₂ ultrathin nanosheets with additional active edge sites for enhanced electrocatalytic hydrogen evolution. Adv. Mater. (40), 5807–5813. https://doi.org/10.1002/adma.201302685.
- Xu, X., Yang, W., Yang, F., Hou, L., Li, Y., 2016. Highly active and reflective MoS₂ counter electrode for enhancement of photovoltaic efficiency of dye sensitized solar cells. Electrochim. Acta 212, 614–620. https://doi.org/10.1016/ielectacta.2016.07.059.
- Yi, M., Zhang, C., 2018. The synthesis of two-dimensional MoS₂ nanosheets with enhanced tribological properties as oil additives. RSC Advance 8 (17), 9564–9573. https://doi.org/10.1039/C7RA12897E.
- Zhang, F., Liang, W., Dong, Z., Niu, Q., Yang, Z., Lin, M., Zhang, J., 2023. Dispersion stability and interfacial properties of modified MoS₂ nanosheets for enhanced oil recovery. Colloids Surf. A Physicochem. Eng. Asp. 675, 132013. https:// doi.org/10.1016/j.colsurfa.2023.132013.